

A New Model of Solar Neutrinos in Manifest Violation of CPT Invariance

R. S. Raghavan

Bell Laboratories, Lucent Technologies, Murray Hill NJ 07974 USA
 INFN Laboratori Nazionali del Gran Sasso, Italy

September 25, 2017

Abstract

The large mixing (mass) (LMA) -MSW model of solar neutrinos (ν_e) is now widely held to be near definitive, based on global consistency with data. No physical effect, however, compels its *uniqueness*. The present search for an explicitly testable competitive model was stimulated by a surprising finding— the high energy part of the standard solar model (SSM) ${}^8\text{B}$ ν_e spectrum can be scaled very precisely to observed flux levels *without measurable shape distortion* via sensitive combinations of long wavelength flavor conversion in vacuum and a ${}^8\text{B}$ ν_e flux $\phi(\text{B}) < \phi(\text{B: SSM})$. Pursuantly, a new “astroparticle” model with the relatively specific parameters $\Delta m^2 = 76 - 78 \mu\text{eV}^2 (10^{-12} \text{ eV}^2)$; $\sin^2 2\theta = 0.58 - 0.56$; $\phi(\text{B}) = 0.83 - 0.81 \phi(\text{B: SSM})$ coupled with modest changes in the SSM, offers a viable solution consistent with data. Because KamLAND has set $\Delta m^2 \sim 50 \times 10^6 \mu\text{eV}^2$, $\sin^2 2\theta \sim 1$ for *antineutrinos*, our model manifestly violates CPT invariance. The model predicts new distortional effects in solar neutrino spectra via ν_e -e scattering signals in the window 3–5 MeV, even though the spectrum is flat above 5 MeV. This window is accessible to experiment for the first time in KamLAND. New experiments are proposed to observe the more dramatic charged-current spectral effects.

1 Introduction

Experimental data on solar neutrinos (ν_e) has accumulated rapidly in the last few years by the operation of several large detector facilities such as Super-Kamiokande (SK), the Sudbury Neutrino Observatory (SNO) and KamLAND. The data from these detectors were precise and informative. The neutral current signals (NC) from ${}^8\text{B}$ neutrinos in SNO [1] showed that ν_e flavor was not conserved because the flavor-blind NC rate explicitly exceeded the charged current (CC) ν_e signal rate. The absolute NC rate was close to the ${}^8\text{B}$ ν_e flux of the Standard Solar Model (SSM)[2]. The (ν -electron) scattering (ES) signal in SK [3] indicated the *type* of flavor conversion with a highly precise energy-independent ES spectrum

in the measured window 5-15 MeV. This result severely restricted the possible ν_e models. Global analyses of solar ν_e data pinpointed matter conversion (MSW effect) in the large mixing (mass) (LMA-MSW) regime as the most favored model of solar neutrinos[4]. Finally, KamLAND observed oscillations of *terrestrial antineutrinos*[5]. The resulting parameters were approximately consistent with LMA-MSW neutrinos, as expected by the invariance of CPT symmetry. The solar neutrino problem therefore appears resolved.

In view of the preponderance of evidence of global consistency for the LMA-MSW model, why search for an alternate model? In principle, however, no physical effect specific to LMA has yet been observed to prove its *uniqueness*. The NC/CC result from SNO[1], shows only that the ν_e 's oscillate but it does not specify the mechanism as LMA-MSW. The lack of a uniqueness proof becomes a central issue (not just a point of principle) if an *explicitly testable* competitive model can be invented.

In this work I show that such a solar neutrino model can be constructed. The uniqueness of *this* model can be proved or disproved by a variety of effects at signal energies <5 MeV. In particular, in contrast to LMA-MSW, sizable shape distortions are predicted in the 3–5 MeV window in ES spectra even though the shape is still flat above 5 MeV. Such an effect in solar neutrino spectra is predicted for the first time. The 3–5 MeV window is now experimentally observable for the first time in a liquid scintillation device such as the already operational KamLAND detector; thus, the above prediction can be readily subjected to experimental test.

The physical mechanism of the present model is long wavelength oscillations (LWO) in vacuum, discovered by a new approach based on “spectral engineering”. Although the underlying parameters were previously detected in the general dragnet of global analysis programs [6, 7] the *experimental effects* of the model are new, unsuspected and distinctly different from those of generic vacuum oscillations.

The ν_e parameters of the model, very different from LMA, imply manifest violation of CPT invariance in view of the KamLAND results. Whether this is a fatal flaw is at present unclear from the standpoint of basic theory. The suggested experimental tests of the new model, however, offer a decisive resolution of the question, thus they are doubly important.

The present work has its origins in a question posed in 1994, if it was possible to conceive a neutrino oscillation model elusive enough to *escape* detection in experiments at the time. The answer was yes, if solar neutrinos oscillated at only the lowest energies. In very long wavelength (VLWO) oscillations in vacuum

with $\Delta m^2 < 10\mu\text{eV}^2(10^{-12}\text{eV}^2)$, ^8B neutrinos are hardly converted; neutrinos < 1 MeV are converted, and explain the ^{71}Ga results[8]. Thus, the ^8B flux deficit observed in the ^{37}Cl data can only be produced by an initial flux *reduced astrophysically to $\sim 1/3$* . This scenario, called “Just-so 2”[9], was the first model to be ruled out [10] by the SNO NC result – the initial flux is apparently the full SSM flux, thus, *conversion* is centrally responsible for the flux deficit. Such an effect is available via LMA-MSW especially since it also supplies the crucial undistorted SK spectrum. Thus, conversion models at two extremes produce the observed undistorted ^8B spectrum in principle, via: 1) VLWO with no ^8B ν_e flavor conversion but a flux reduction by a factor ~ 0.36 ; and 2) LMA-MSW with ν_e survival of ~ 0.36 but the full initial SSM ^8B flux.

The question then arises whether a scenario could be engineered with a *mixture* of *both* flavor conversion *and* a smaller initial flux that leaves the high energy part of the ^8B ν_e spectrum *shape invariant* so that all the experimental consequences (at > 5 MeV) follow automatically. By definition, this does need a smaller initial ^8B flux than the SSM/SNO value, however, in the spirit of global analyses made so far, one could tolerate in principle a lower flux up to the 2σ lower limit of the SNO NC result, i.e., $> 75\%$ of the SSM flux.

The surprising initial discovery was that a shape invariant high energy ^8B neutrino spectrum could indeed be engineered to a high degree of precision (within a few percent) by a sensitive choice of the initial flux and mass-mixing parameters in a very narrow band $\Delta m^2 = 70\text{-}80 \mu\text{eV}^2$, ~ 10 times larger than the VLOW-just-so2 regime [8]. The oscillations in the new regime are thus termed long-wavelength or LWO in this paper. The new mass-mixing band is very different from LMA-MSW regime. In view of the KamLAND result, one thus immediately faces the problem of violation of CPT invariance by neutrinos. Nevertheless, work proceeded undeterred. Recent theoretical ideas appear to allow that the otherwise rigid invariance of CPT may be relaxed in principle in the neutrino sector[11].

2 Spectral Engineering

Fig.1 illustrates the central thesis of this work. It shows a series of ^8B ν_e spectral shapes engineered via LWO to reproduce at high energies, the rate and shape of the LMA-MSW (thick red) solution as closely as possible. The LMA shape is defined as the standard SSM shape (thin blue) scaled by the factor 0.365 (0.349(22), the CC flux at SNO). The convenient definition “LMA = 0.365 SSM” agrees very closely in the $\phi(^8\text{B})$ and the flat spectral shape observed above 5 MeV. The other

spectra are derived with “shape invariant” LWO parameter combinations (see box and caption of Fig.1) chosen individually and interactively on-line.

The shapes change extremely sensitively with the three ν_e parameters that tune up a viable solution systematically: The Δm^2 arranges the flavor survival P_{ee} spectrum such that a roughly horizontal part energywise, is positioned in the >5 MeV regime; the $\phi(B)$ parameter scales it into the LMA shape window; the $\sin^2 2\theta$ that strongly affects the curvature, flattens it into a nearly undistorted shape. The final angles that expose the new model are in general, smaller than previously examined; e.g., solutions with the same $\Delta m^2 = 76 \mu eV^2$ but $\sin^2 2\theta \sim 0.8$, beyond the present range ≤ 0.58 , failed earlier [12] and in this work.

Fig. 1 shows that the needed shape invariance can be achieved with precision above ~ 8 MeV below which the LWO shapes fan out deviating from the LMA-MSW shape. We aim at neutrino reaction signals such as ES and $CC > 5$ MeV using these input shapes. Thus, deviations in Fig 1 between 5 and 8 MeV appear problematic. In both ES-SK and CC-SNO that apply the Cerenkov technique, the experimental signals of the electron kinetic energy T range above 5 MeV. In the quest for LWO ν_e shapes that generate ES/CC shapes that fit the data, the spectral smearing due to the inherent reaction as well as the detector energy resolution play a key role. In the end, for both CC and ES, the overall spectral smearing is such that the dominant contribution to the ES and CC signal comes from $E(\nu_e) > 8$ MeV where the spectral match is close. The possible deviations occur mainly near the 5 MeV signal threshold where background is strong in both SK and SNO.

This effect can be understood in the case of the ES shape since the ES signal at a given electron energy is derived from the whole neutrino spectrum above that energy, i.e. the reaction smearing effect is complete[13]. Even a large deviation e.g., at 5–6 MeV is damped down considerably in the ES spectrum. In the case of the CC spectrum $T > 5$ MeV which implies $E(\nu_e) > 6.44$ MeV, the deviations look more worrisome since in this case one normally expects 1-to-1 correspondence of $E(\nu_e)$ and T, thus no reaction smearing. In reality, there is considerable reaction smearing even for the CC signal since in the reaction $\nu_e + d \rightarrow 2p + e$, the proton recoils cannot be neglected[14]. The effect removes the $E(\nu_e)$ -T correspondence significantly (although not to the extent in ES). The final effect is shown in Fig. 2 where the light blue curve for no recoil corrections peaks at 8 MeV. The recoil correction results in a large downshift to < 7 MeV. The detector resolution smearing produces a further downshift to ~ 6.5 MeV. Thus, also the CC signal shape is determined largely by $E(\nu_e) > 8$ MeV.

The plan of search for a new ν_e model was as follows. In the first step, the viable basic parameters of the LWO scenarios were fixed by matching predicted

shapes and rates to the ES-SK result, by far the most the stringent test. The ES spectral/rate match set the primary fix of the $\sin^2 2\theta$ and $\phi(\mathbf{B})$ values for each selected Δm^2 in the viable band. The match to the SNO CC data followed with the same parameter set except for possibly very slight changes in the scaling $\phi(\mathbf{B})$ only. With a reasonable match to data on ν_e (^8B), the matches to low energy data from ^{37}Cl and ^{71}Ga were tested with the same final set of parameters reached above. The upper limit of the Δm^2 band is $\sim 80\mu\text{eV}^2$, because, beyond this limit, the spectral deviations around 5 MeV become too large to accommodate a spectral match to the data. At $\sim 70\mu\text{eV}^2$ and below, the required scaling factor $\phi(\mathbf{B})$ dips < 0.75 , the 2σ limit of SNO.

3 Electron Scattering

The procedure involved the calculation of the ES spectra for LMA and LWO scenarios normalized to that for the SSM spectrum with no conversion. Thus, the ES signal for each scenario is:

$$R(\text{ES}) = [\langle W(\lambda; P_{ee}) + Z(\lambda; 1 - P_{ee}) \rangle] / \langle W(\lambda) \rangle \quad (1)$$

where W and Z are the differential ES cross-sections for e^- and μ/τ neutrinos respectively [13], averaged over the SSM ν_e spectrum $P(\lambda)$ [13] modified by the e -flavor survival function P_{ee} that, in general, depends on $E(\nu_e)$. The $\langle \rangle$ in (1) indicate convolution with the detector resolution in SK[15].

For the LMA case, P_{ee} is a *constant* $= 0.365$, close to 0.349(22) (relative to the SSM flux of $5.05 \times 10^6 \text{ cm}^2\text{s}^{-1}$), the value found in CC-SNO. Then, $W(\lambda; P_{ee}) = W(\lambda) \times 0.365$ and $Z(\lambda; 1 - P_{ee}) = W(\lambda)(1 - P_{ee})0.16 \approx W(\lambda) \times 0.635 \times 0.16$, because of the nearly constant value of $Z/W \approx 0.16$ for solar ν_e energies > 3 MeV. This leads to $R(\text{ES}; \text{lma}) 0.466 \approx 0.465(15)$, the SK result [3] relative to the SSM flux above (the reason for choosing $P_{ee}(\text{LMA}) = 0.365$).

In the case of the LWO spectra, the same procedure was used. Here P_{ee} is energy dependent, given by the standard oscillation formula for solar baseline:

$$P_{ee} = 1 - \sin^2 2\theta \sin^2 \{0.1899[\Delta m^2(\mu\text{eV}^2)/E(\nu_e)(\text{MeV})]\} \quad (2)$$

For each value of Δm^2 , using the convoluted spectra $\langle W(\lambda; P_{ee}) + Z(\lambda; 1 - P_{ee}) \rangle$ and $\langle W(\lambda) \rangle$, the ES signals were calculated as in (1).

This spectrum (energy dependent in principle), was matched to the data points of the ES-SK spectrum [16] by varying the parameters $\phi(\text{ES})$ (< 1) and $\sin^2 2\theta$

for each value of Δm^2 in the range 70-80 μeV^2 . The best match was selected interactively for a given value of Δm^2 from the χ^2 of the fit of the R(ES) curve to the ES-SK data points. The results are shown in Fig. 3.

The box in Fig. 3 shows the values of the parameter combinations [Δm^2 ; $\sin^2 2\theta$; $\phi(\text{ES})$], “the “best match” [χ^2] (dof =16 for 17 SK data points in the range 5-14 MeV) and the [R(ES) area] normalized to SSM for each curve including ES-lma. The ES(lwo) curves are seen to match the SK data, particularly those for $\Delta m^2 = 75\text{-}78 \mu\text{eV}^2$, even in the narrow slit allowed by the high statistical precision of the SK data. Indeed, except for the first two data points at the lowest energies in Fig. 3 that are the most susceptible to background, the χ^2 values (dof =14) for T= 6.5–14 MeV (also given in the box in Fig 3) for $\Delta m^2 = 75\text{-}78 \mu\text{eV}^2$ jump to 1.05 to 1.15 with probabilities in the range of 35% compared to the best fit 50% value for $\chi^2=1$. The rate matches are excellent (see Table 2 below). Our new model thus passes its most severe test. A key reason is the significantly smaller mixing angles used here (compared to previous analyses) that flatten the ES spectra sufficiently to be scaled into the ES data window. Another key effect is detector resolution as shown in Fig. 4. The unconvoluted ES(lwo) curve (in blue) with a discouraging shape (even without the low energy points) reduces to the much more acceptable curve (in red) that includes the effect of the SK energy resolution.

4 CC Reaction on deuterons

The CC reaction $\nu_e + d \rightarrow 2p + e$ has been applied at SNO to measure directly the ν_e ^8B spectrum. The theoretical cross sections for this reaction including the recoils of the two protons in the final state have been extensively tabulated[17]. The calculation of the CC spectra for LWO and LMA, input ν_e spectra must be summed over the contributions of ν_e from 0 to $E(\nu_e)(\text{max}) = T + Q (=1.44 \text{ MeV})$ for each signal electron kinetic energy T instead of just from the single ν_e energy T+Q. The cross section $C(\lambda; P_{ee})$ is first averaged over the input solar ν_e spectrum $P(\lambda)$ modulated by the P_{ee} of the oscillation scenario. $P_{ee}(\text{LMA}) = 0.365$. $P_{ee}(\text{LWO})$ is given by (2). For each value of Δm^2 the CC shapes were generated as:

$$R(\text{CC}) = \phi(\text{CC}) \langle C(\lambda; P_{ee}) \rangle \quad (3)$$

where P_{ee} was calculated with the same mixing parameter fixed in the ES-SK spectral match. The $\langle \rangle$ indicates, as before, convolution with the SNO detector resolution[1]. $\phi(\text{CC})$ is the scale factor applied to match the LWO-CC spectrum

to LMA-CC spectrum measured at SNO. The shape matches aimed at fits (by eye) within a $\pm 12\%$ band, the error band in the measured SNO-CC spectrum[1]. Fig. 5 shows the LWO-CC matches to the LMA-CC spectrum (thick red line marked SSM*0.365). The legend box shows in [] the signal areas under the curves in the window 5–13.5 MeV.

The scale parameter $\phi(\text{CC})$ is the true flux of $\nu_e(^8\text{B})$. The spectral matches in Fig. 5 are good with only a $\sim 10\%$ deviation even at the lowest energies that are most susceptible to errors from background and the disentanglement of the relatively broad NC γ -ray shower signal that occurs at the effective energy of ~ 5 MeV instead of at its full energy of 6.15 MeV[18]. The rate matches are also good (see Table 2). The best match LWO parameter group in the CC matches as well as overall, is $[\Delta m^2 (\mu\text{eV}^2)/\sin^2 2\theta/\phi(\text{CC})] = [77/0.57/0.82]$.

5 Low Energy Signals from ^{37}Cl and ^{71}Ga

We now consider how the low energy parts of the new model, constructed so far only with high energy ^8B solar neutrinos in mind, match the signals from the ^{37}Cl and ^{71}Ga detectors that respond not only to the low energy parts of the ^8B spectrum (^{37}Cl Q=0.814 MeV) but beyond, to the lowest energies of the pp ν_e 's (^{71}Ga Q=0.235 MeV).

Interaction rates (in SNU= 10^{-36} /target nucleus/s) were calculated using well-known target data and standard ν_e spectra from every solar source [19] modulated by the LWO effect using (2). Table 1 lists these results for ^{37}Cl and ^{71}Ga for the SSM as well as LWO with the same parameters fixed by the ES and CC-matches above. The values for the SSM agree with published values[2], checking the overall source data and the calculation methods.

Table 1 shows the signal rates in the lines marked “Total SNU” in 4 different *solar astrophysical* scenarios. These rates compare with the measured SNU for Cl and Ga (last line in each section). The favored LWO groups are highlighted. The first result is the line marked SSM, for the standard sun. The LWO results for Ga range between ~ 80 –82 SNU that deviate by $\sim 2\sigma$ from the measured value of 70.8(44) SNU[20]. The match of LWO rates with the Cl data, 2.56(23) SNU[21], is worse, deviating systematically from it by $> 3\sigma$ for every LWO parameter choice. A similar problem exists *also for the LMA-Cl match* (see Table 2 below). The fact that the mismatch in Cl is much worse than in Ga indicates that problem lies in the spectral region between 1–5 MeV. Neutrino spectral engineering cannot solve this problem.

Astrophysical spectral adjustments, on the other hand, could be resorted to, to a limited extent by changes in the solar fluxes. The only negotiable fluxes in the framework of the SSM are the ${}^8\text{B}$ flux (predicted with a large error $\sim 20\%$) and the CNO fluxes ($\sim 100\%$)[2]. Two astrophysically sound remedies touching these solar sources are conceivable.

The LWO scenarios above are based inherently on the assumption $\phi(\text{B}) < \phi(\text{B:SSM})$. This idea must be astrophysically based, not stand as an ad hoc construct as tacitly viewed so far. The simplest way to reduce the ${}^8\text{B}$ flux is to reduce the central temperature T of the sun using astrophysically sound scaling laws: $\phi(\text{B}) \propto T^{20}$ and $\phi(\text{Be}) \propto T^{10}$ [22]. Using the matched values of $\phi(\text{CC-B})$ above ($\sim 71\text{--}80\%$), the reduction in $\phi(\text{Be})$ can be calculated. This correction is applied in the lines marked SSM(T) in Table 1. The correction helps to a small extent.

The second remedy concerns the CNO flux for which there is little astrophysical guidance. Global fits of all neutrino scenarios proposed so far are eminently compatible with 0–5% CNO luminosity in the sun[23]. We therefore suggest that the CNO flux is seriously reduced, viz. $=0$. The lines marked (No CNO) reflect this assumption. This correction helps substantially in the LWO-Cl match. Finally both astrophysical modifications result in the rates marked SSM [No CNO(T)]. The Cl rates now match the LWO predictions within 1.65σ (similarly, no-CNO helps *also the LMA-Cl* match to move within 1.5σ , see Table 2) The LWO Ga match also improves to a much closer $\sim 0.3\sigma$. We therefore accept and *require* these astrophysical modifications; hence the designation “astroparticle” to our model.

Table 1 indicates the reason why Δm^2 values below $75\mu\text{eV}^2$ become rapidly untenable. The LWO oscillations become progressively faster as $E(\nu_e)$ decreases (see Fig. 1). At the energy of the ${}^7\text{Be}$ line (0.862 MeV), the oscillation period changes rapidly with Δm^2 . Below $75\mu\text{eV}^2$ the Be line strobos into a resonance, thus P_{ee} jumps to ~ 1 . The Be contribution to the Cl (as well as the Ga) rate jumps, causing both to fall out of match. Even though the LWO- ${}^8\text{B}$ matches are good for $85 > \Delta m^2 > 70\mu\text{eV}^2$ the Be factor limits the model at $\Delta m^2 = 75\mu\text{eV}^2$ as long as $\phi({}^8\text{B}) \geq 0.8 \phi({}^8\text{B:SSM})$.

6 Model & Data

The discussion above has examined in detail the compatibility of the predictions of the new LWO-based astroparticle model of solar neutrinos to every experimental result available to date with sensitivities that span the entire solar neutrino

spectrum. In Table 2 we summarize the match of model to data quantitatively and individually. The “astroparticle LWO model” is competitive with the (astroparticle) LMA in the consistency with the global data. The major difference is a 1.4σ mismatch with the SNO *absolute NC rate*, a main reason why the LWO scenario was disfavored in global analyses such as [6] even though it was found competitive in the absence of the NC result.

7 Experimental tests

For the LMA-MSW, *only* two types of experimental data can provide new support. The first is a substantial improvement in the precision of the absolute NC signal rate. We note that the fundamental difference *vis a vis* the LWO model is a mere 20% lower ${}^8\text{B}$ ν_e flux. The NC rate in SNO is now known to $\pm 13\%$ 1σ [1]. This precision needs to improve markedly to exclude the possibility of a 20% lower flux by at least 3σ . The second possibility is the only predicted effect specific to the LMA *viz.*, a gradual rise of the CC signal from 0.365 SSM above 5 MeV to 0.6 SSM below 1 MeV in the region of the ${}^7\text{Be}$ and pp neutrinos[24]. This regime, endemic to high background is difficult to access experimentally and the LMA vs. LWO test requires sharp differentiation of somewhat comparable signals at 0.6 SSM and 0.45 SSM (see last lines in Table 1) respectively. The first opportunity for this test will arise when Borexino[25], designed for very low background at low energies, starts operation in 2004. We now turn to experiments aimed specifically at exposing the LWO basis of the new model.

8 ES Signals at KamLAND, BOREXINO

The basic premise of the present model is spectral shape invariance for $E(\nu_e) > 5$ MeV under the action of LWO. However, as seen in Fig. 1 this action is fundamentally accompanied by *strong shape changes immediately below 5 MeV*. Experimental tests accessible to the signal window < 5 MeV, hitherto unexplored via direct solar neutrino detection, hold the key to a compelling demonstration of the present model since the LWO spectral predictions in this window are dramatically different from the relatively weak shape effects in the LMA case. This window is closed to the present large-scale Cerenkov detectors SK and SNO. It is however accessible to a liquid scintillator (LS) based detector on the scale of at least 1 kton target mass (similar to SNO though much smaller than SK with 22 kton fiducial

mass). KamLAND is such a detector that is already operational[3]. Borexino is another, that will soon be operational. Both are designed for low background neutrino spectroscopy at low energies, a key factor in considering signals below 5 MeV. We first consider KamLAND because interesting data can be expected from this device in the very near future.

Let us first consider ES signals below 5 MeV. Fig. 6 shows the ES spectra expected in a 1 kton LS detector. These are theoretical curves unconvoluted with detector resolution since the superior energy resolution in a LS device results in little smearing of the spectral shapes. Fig. 6 shows that while the ES spectra for LMA and LWO match identically above 6 MeV, they diverge significantly below this critical energy. While it is obviously desirable to measure the full spectrum and determine the shape characteristics below 6 MeV (normalized to the “flat” part >6 MeV), a reliable preliminary indication of the effect can be obtained just from the relative rates in two broad windows below and above 6 MeV. Table 3 lists the signal rates/2y live time for the two models in the windows 3–6 and 6–16 MeV. In the LWO scenario (with practically no differences between the viable solutions), the excess of counts at 3–6 MeV is measurably higher than in LMA, 484(39) vs. 370(38), a $\sim 3\sigma$ effect. For the lower threshold at 2.5 MeV background permitting, the LWO effect can possibly be detected at the $\sim 4\sigma$ level. KamLAND has been in operation now for nearly two years but it is not clear if data on signals in these windows are available. Information is therefore eagerly awaited.

In KamLAND the background characteristics in the 2–5 MeV regime, the key factor, is not known. The relatively shallow depth of this detector could pose a high cosmogenic background interference. In Borexino, with a larger overburden, this problem is less acute. The disadvantage is that in the present design, the largest mass available in Borexino is only 300 tons[25]. It is envisioned that the target mass can be upgraded to approach 1 kton in the future, when a definitive result on LWO can be attempted.

9 ^7Li CC Spectroscopy

The ES spectra in Fig. 6 are interesting and informative especially since they may be observable already in KamLAND. However, the spectral effects are considerably less prominent than could be expected from Fig. 1 because of the basic spectral smearing effect of the ES reaction (although the less serious detector smearing is avoided). One can thus expect stronger effects in CC transitions with bound

nuclei in the final state that ensure that the signal electron energy is uniquely connected to the ν_e energy (unlike in the ν_e+d reaction). Other considerations in the choice of the reaction are: 1) a high rate and/or a large target mass since the ${}^8\text{B}$ ν_e flux is small and 2) a low threshold. The latter is important since an energy threshold >3 MeV is desirable in order to avoid background. An ideal choice is the case of ${}^7\text{Li}$, long known as a candidate for direct solar neutrino spectroscopy [26] but not so far applied in practice.

Fig. 7 shows the nuclear data relevant to the inverse $\beta(\text{IB})$ reaction $\nu_e+{}^7\text{Li}\rightarrow{}^7\text{Be}+e$. The IB threshold is only 0.862 MeV so that dominant part of the ${}^8\text{B}$ ν_e spectrum can be observed above a ~ 3 MeV signal threshold. The IB transition is a superallowed transition with a precisely calculable rate, one of the highest known in beta decay. As a light nucleus with a high natural abundance, a relatively small mass of 30–100 tons (compared to 1 kton) may suffice for a decisive result. Technical details are beyond the scope of this paper, but a suitable technology for the Li-CC experiment appears possible.

Fig. 8 (left) shows CC spectra observable in the Li IB reaction. Almost the entire spectrum occurs above 3.5 MeV, comfortably above the background threshold. With the thick red line for $\text{SSM}\cdot 0.365=\text{LMA}$ as the reference, the spectra directly display the essential action of Fig. 1, –shape invariance above 8 MeV and dramatic modulation at lower energies. The prominence of the modulations is illustrated in Fig. 8 (right) where the LWO spectra are normalized to LMA which appears as a flat line. The spectral deviations are strong and compelling. Table 4 lists the signal rates in two broad windows above and below 7 MeV. The yearly rates are high. In the low window, the LWO rates are $\sim 50\%$ higher than the LMA, whereas in the high window they are same (within $\sim 3\%$). It would thus appear that the essential proof of the LWO basis of the present model could be obtained in one year’s live time possibly with a target mass as small as 30 tons of Li.

The LWO modulations become even stronger at very low energies in regime of the pp neutrinos. Even in the relatively small window of a few hundred keV several periods of LWO modulations occur. These modulations *may* be observable by a suitable CC transition with a sufficiently low threshold that can be implemented by a technology that offers sharp energy resolution. The modulations at these energies are more sensitive to the neutrino parameters than at the high energy windows considered above. Thus it may be possible to determine them more precisely than the narrow LWO specifications already inherent in the present model. An ideal choice for this application is the CC transition in ${}^{115}\text{In}$ [27]. A practical real time pp neutrino detector based on indium is under development in the LENS project [28]. The application of LENS to the spectroscopy of the present neutrino

model will be discussed elsewhere.

10 Conclusions

Is the LMA-MSW model the last word in solar neutrinos? It may well be. The present work raises a serious possibility that it need not *necessarily* be. We have made the *prima facie* case that a model based on LWO, a very different physics scenario, offers a credible alternative. Only a 20% difference in a measured absolute signal rate stands between them. The serious pause against the new model is, clearly, the possible violation of CPT invariance that may hold rigidly also in the neutrino sector in spite of recent suggestions to the contrary. It is thus a classic case of decision by a unique physical result vs. discovery by consensus with a mass of different data. Experiments with the potential for compelling spectral impact are proposed in this work and may already be observable. Only they can tell which model is the prevalent one.

The impact of this decision goes well beyond the already rich field of solar neutrinos. This science has led us deep into the sun's interior and beyond the Standard Model of particle physics. Is it poised to take us to yet more unknown territory opened by the breakdown of one of the most cherished symmetry principles in physics?

11 Acknowledgments

I wish to express my sincere thanks to Peter Kurcynski who initiated me into the mysteries of MS-EXCEL computing used extensively in this work and for helpful discussions. I am grateful to K. Kubodera and S.Nakamura for generously supplying their tabular data in a format ready for use in this work. I thank John Bahcall, Michel Cribier, Eligio Lisi, Sandip Pakvasa and Carlos Peña-Garay for their comments on the draft MS.

References

- [1] Q. R. Ahmad et al, Phys. Rev. Lett. **89**, 011302, 2002; nucl-ex/0204008
- [2] J. N. Bahcall, M H. Pinsonneault and S. Basu. Ap. J. **555**, 990, 2001; astro-ph/0010346

- [3] S. Fukuda et al, Phys. Lett. **B359**, 179, 2002; hep-ex/0205075
- [4] See S. Pakvasa and J. W. F. Valle, hep-ph/0301061, for a review of global analyses of solar neutrino data by different authors.
- [5] K. Eguchi et al, hep-ex/0212021
- [6] See for example, G. L. Fogli et al, hep-ph/0206162. In this paper, the new model described in the present work was allowed in the absence of the SNO NC data but disfavored at 3σ after the NC data (see Section 6).
- [7] P. I. Krastev and S. T. Petcov, Phys. Rev.**D53**,1665 (1996; hep-ph/9510367. This paper and [8], first considered the effect of $\phi(^8\text{B}) < \phi(^8\text{B:SSM})$ which revealed the possibility of very low Δm^2 solutions. The conclusions were only qualitative in the current context since these works considerably pre-date precision results from SK and SNO. These papers showed that shape distortions occur at pp-neutrino energies. They did not point out the crucial medium energy shape effects brought out in the present paper.
- [8] R. S. Raghavan, Science **267**, 45 (1995).
- [9] J. N. Bahcall, P. Krastev and A. Yu. Smirnov, J. H.E.P. **5** , 015, 2001; hep-ph/0103179
- [10] V. Barger et al, Phys. Lett. **B537**, 179, 2002; hep-ph/0204253
- [11] G. Barenboim, L. Borisso and J. Lykken, hep-ph/0212116; G. Barenboim et al, hep-ph/0108199; H. Murayama and T. Yanagida, hep-ph/0010178.
- [12] For example, Y. Suzuki, Nucl. Phys.(Proc. Suppl) **B77**, 35, 1999
- [13] J. N. Bahcall , *Neutrino Astrophysics* (Cambridge) 1989
- [14] J. N. Bahcall and E. Lisi, Phys. Rev. **D54**, 5417 1996
- [15] The detector resolution function at SK was kindly supplied by M.Nakahata.
- [16] M.Vagins, Talk at Conference on “*Neutrino News from the Lab and the Cosmos*” Fermilab, Oct 2002. The data points of the ES-SK spectrum were transcribed from a transparency of this talk downloaded from the Web.
- [17] The Tables of differential cross-sections of $\nu_e + d$ prepared by K. Kubodera, S. Nakamura et al were kindly sent to me by S. Nakamura.

- [18] M.Chen , Private communication
- [19] Data generously posted by J. N. Bahcall on his website:
www.sns.ias.edu/~jnb/
- [20] The cited value is the combined result of SAGE and GALLEX/ GNO as given in ref. 6.
- [21] B. T. Cleveland et al, Ap. J. **496**, 505, 1998.
- [22] G. Fiorentini and B. Ricci, hep-ph/9509429.
- [23] J. N. Bahcall, M. C. Gonzalez-Garcia and . C. Pena-Garay, astro-ph/021331.
- [24] J. N. Bahcall and P. Krastev and Au. Y. Smirnov, Phys. Rev **D58**, 096016, 1998; hep-ph/9807216
- [25] Borexino Collaboration, Astroparticle Phys. **16**, 215 2002
- [26] F. Reines and R.M. Woods, Phys. Rev. Lett. **14**, 20, 1964; F. Reines, Proc. Roy. Soc. **A301**, 159, 1967.
- [27] R. S. Raghavan Phys. Rev Lett. **37**, 259, 1976; hep-ex/0106054 June 2001.
- [28] Status Report on LENS –10/02, R. S. Raghavan (for the LENS Collaboration), Report to the LNGS -Gran Sasso Laboratory Scientific Committee, Oct 2002 (available from LNGS Library).

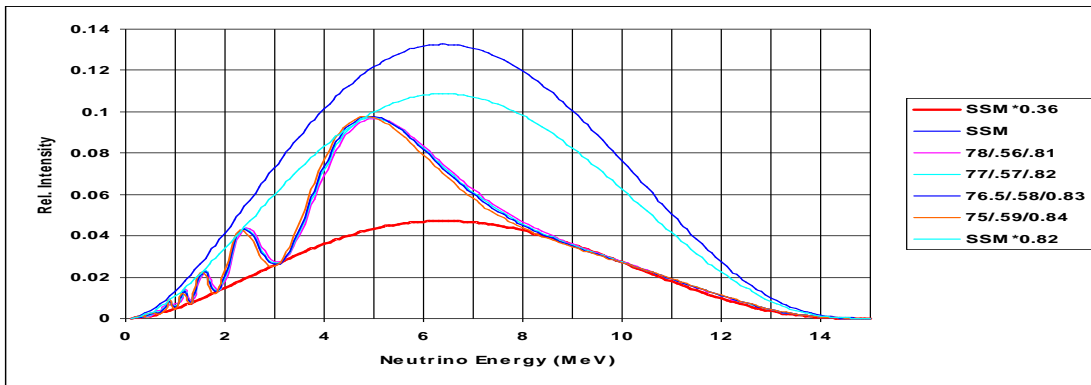


Figure 1: ^8B Solar neutrino spectra under different LWO scenarios (the parameter combinations $[\Delta m^2(\mu\text{eV}^2)/\sin^2 2\theta/\phi(\text{B})]$ (fraction of $\phi(\text{SSM})$) are listed on the right). The spectra are engineered to produce a “shape invariant” high energy part. The central curve (red) is the LMA-MSW $\equiv 0.365\phi$ (B:SSM).

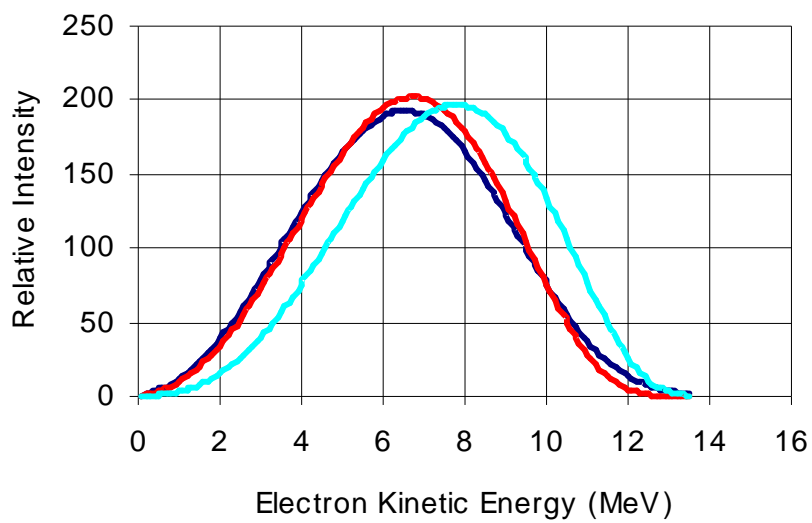


Figure 2: CC spectral shapes from $\nu_e+d \rightarrow 2p+e$ in SNO with 1) no recoil or detector resolution (light blue); 2) recoil only (red) and 3) recoil and resolution corrections (final experimental shape; dark blue).

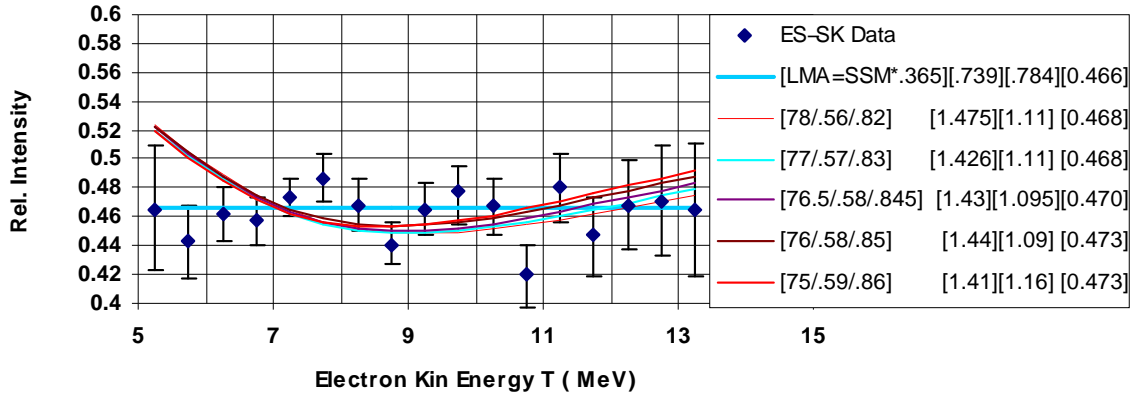


Figure 3: R(ES) spectra of LWO matched to ES data points from SK. The legend box lists the parameter groups: 1) the best match ν_e parameters $[\Delta m^2(\mu\text{eV}^2)/\sin^2 2\theta/\phi(\text{ES})]$; 2) the $[\chi^2]$ values of the fit to the ES-SK data points in the energy range 5-14 MeV; 3) $[\chi^2]$ for the fit in the range 6.5-14 MeV; and 4) the area of [R(ES)] as fraction of the SSM flux assuming no oscillations. LMA = SSM*0.365 leads to the result R(ES-LMA)=R(ES-SK)=0.466.

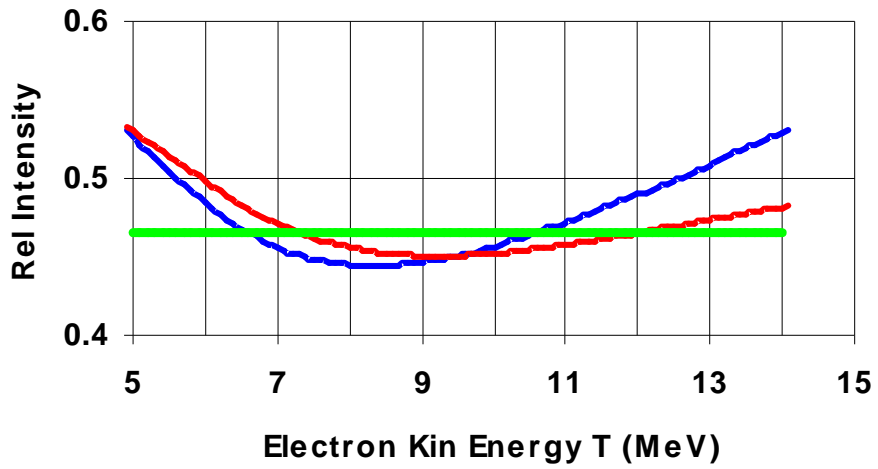


Figure 4: Effect of detector resolution (SK) on ES(lwo) spectrum (blue). The convolution improves the match of the observed spectrum (red) to ES(lma) (green).

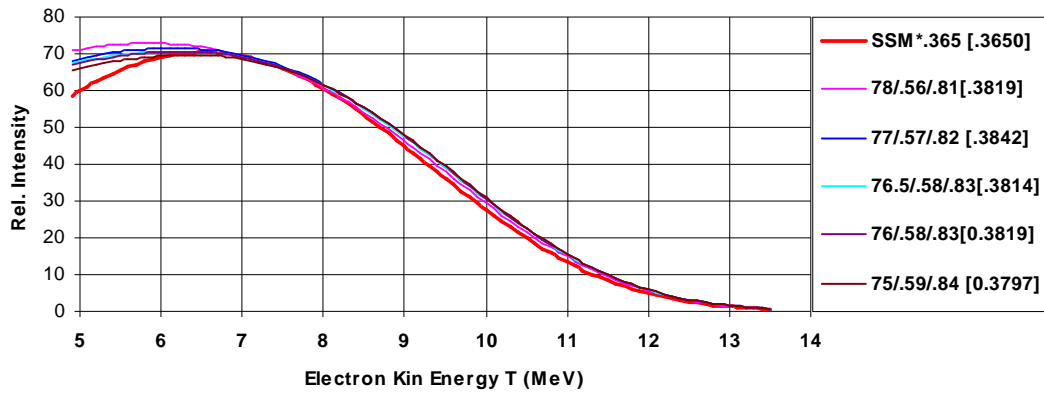


Figure 5: CC spectra of $\nu_e+d \rightarrow 2p+e$ for LWO models with parameter combinations listed in the box, compared with the prediction for LMA (=SSM*0.365; thick purple line). The SNO-CC measurement observes this curve with an error band $\sim \pm 12\%$ which completely encloses the LWO curves. The areas normalized to SSM are shown in [].

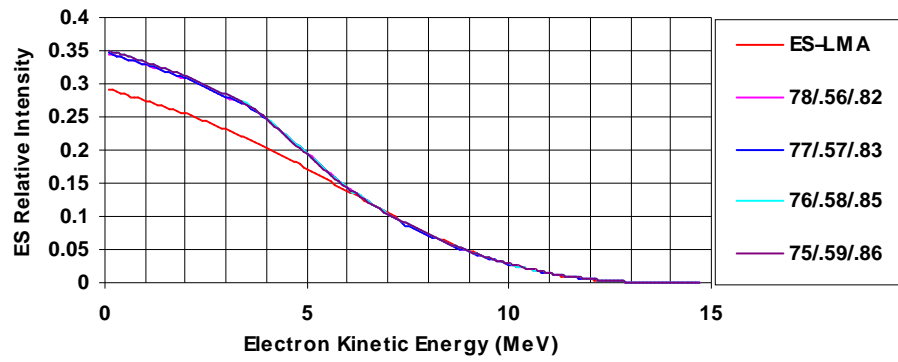


Figure 6: ES spectra predicted for LMA and LWO in the KamLAND liquid scintillation detector. The curves are unconvoluted with energy resolution that is not expected to affect the shapes significantly in KamLAND.

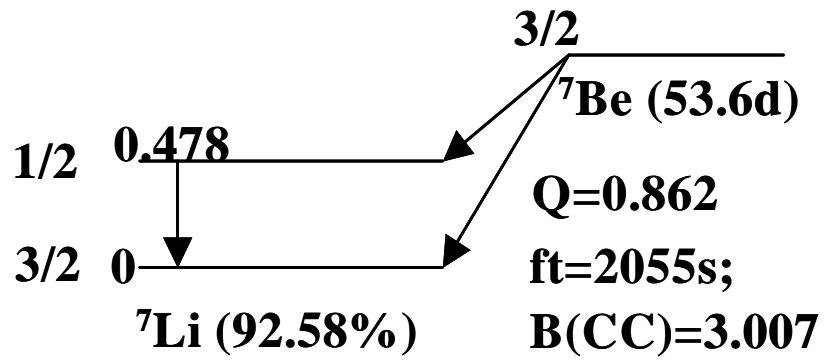


Figure 7: Level scheme of the ${}^7\text{Li}$ - ${}^7\text{Be}$ Inverse β system

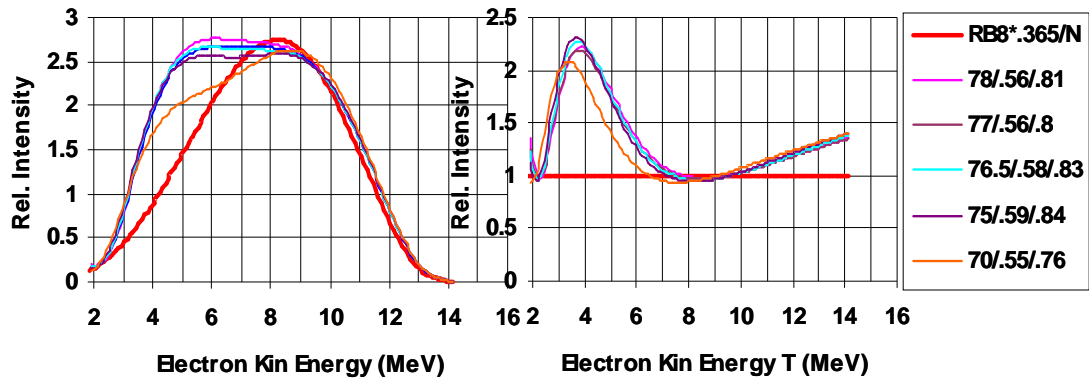


Figure 8: Theoretical CC spectral shapes from the reaction $\nu_e + {}^7\text{Li} \rightarrow {}^7\text{Be} + e$ ($Q=0.862$ MeV) for different LWO parameters and $\text{LMA}=\text{SSM} \cdot 0.365$ (thick red). The panel on the left shows the inverse beta reaction spectra and on the right, the spectra normalized to that of $\text{SSM} \cdot 0.365$.

Table 1: LWO Predictions for the ^{37}Cl and ^{71}Ga solar neutrino detectors. The viable groups are highlighted and the best overall LWO choice is highlighted deeper.

37Cl	Model	SSM	LWO Parameters						
			80/.55/.79	78/.56/.81	77/.57/.82	76.5/.58/.83	76/.58/.83	75/.59/.84	70/.55/.76
	Be	1.15	0.60	0.51	0.55	0.58	0.64	0.77	1.11
	pep	0.22	0.12	0.15	0.15	0.17	0.18	0.19	0.22
	O15	0.33	0.24	0.25	0.25	0.24	0.24	0.24	0.24
	N13	0.10	0.07	0.07	0.07	0.07	0.07	0.07	0.08
	B8SNU	5.76	2.92	2.86	2.81	2.76	2.76	2.71	2.96
	B8x f(B)	5.76	2.31	2.32	2.31	2.29	2.29	2.27	2.25
	Total SNUSSM	7.56	3.35	3.29	3.32	3.36	3.42	3.55	3.89
	Total SNUNoCNO	7.13	3.03	2.97	3.00	3.04	3.11	3.24	3.57
	T(Be/To)=fB^0.05		0.99	0.99	0.99	0.99	0.98	0.99	0.99
	Be(T)=[T(Be)/To]^10		0.90	0.90	0.90	0.90	0.90	0.92	0.87
	Total SNUSSM(T)	7.56	3.29	3.24	3.26	3.30	3.36	3.49	3.74
	Total SNUNoCNO(T)	7.13	2.97	2.92	2.95	2.98	3.04	3.17	3.43
	Measured	2.56(23)							
71Ga									
	B8	12.10	6.97	6.89	6.86	6.55	6.44	6.31	6.28
	B8xf(B)	12.10	5.51	5.24	5.21	5.24	5.15	5.05	4.46
	O15	5.50	4.04	4.08	4.09	4.02	3.99	3.97	3.91
	N13	3.40	2.43	2.45	2.46	2.42	2.41	2.41	2.44
	pep	2.80	1.54	1.91	2.11	2.18	2.27	2.45	2.74
	Be	35.20	18.71	15.88	17.20	17.57	19.01	23.05	33.99
	pp	69.70	50.89	50.24	49.15	48.48	49.04	49.93	48.39
	Total SNUSSM	128.70	83.12	79.79	80.22	79.90	81.87	86.85	95.93
	Total SNUNoCNO	119.80	76.64	73.27	73.67	73.47	75.47	80.48	89.58
	Be(T)=Be(SSM)(T/To)^10	35.20	13.76	14.60	15.76	15.70	17.36	20.50	28.55
	Total SNUSSM(T)	128.70	78.17	78.51	78.78	78.03	80.22	84.30	90.49
	Total SNUNoCNO(T)	119.80	71.69	71.98	72.23	71.60	73.81	77.93	84.14
	Measured	74.1(7)							
	Signal(Be:SSM)			0.45	0.49	0.51	0.55	0.67	0.96
	Signal(Be:T)			0.39	0.43	0.45	0.49	0.60	0.82
	Signal(Be:LMA)			-0.6					

Table 2: Comparison of LWO and LMA vs. Experimental Data

Model Parameters	LWO	LMA≡ SSM*0.365#	Measured Data	σ -LWO	σ -LMA
<i>⁸B Neutrinos >5 MeV</i>					
ES					
Rate (%SSM)	0.468	0.466	0.465(19)*	0.065	0.05
Flat Shape: χ^2 (5-14 MeV)	1.426	0.739			
χ^2 (6.5-14 MeV)	1.1	0.784			
CC					
Rate(%SSM)	0.3842	0.365	0.349(22)*	1.6	0.73
NC					
Rate(%SSM)	0.82	1	1.000(127)	1.42	0.01
<i>Other Neutrinos</i>					
³⁷Cl Rate					
(SSM(T:NoCNO))	2.95	2.91**	2.56(23)	1.69	1.5
⁷¹Ga Rate					
(SSM(T:NoCNO))	72.23	69	70.8(44)	0.32	0.41

At $E(\nu_e) > 5$ MeV there is practically no difference between true LMA and $SSM \times 0.365$

* Relative to BPSSM $\phi(^8B) = 5.05 \times 10^6 / \text{cm}^2\text{s}$

\$ True LMA-MSW

** No CNO only

Table 3: ES Signal rates expected in KamLAND (1 kton liquid scintillator)/2 years live time

Model	R(6-15 MeV)	R(3-6 MeV)	ΔR	R(2.5-6 MeV)	ΔR
LMA*	538	908	$+370\pm 38$	1056	$+518\pm 40$
LWO	536	1020	484 ± 39	1220	$+684\pm 41$

* $SSM \times 0.365$, a sufficiently close approximation in the energy windows considered here.

Table 4: Solar neutrino signal rates/year in low and high energy windows for a 100t Li CC detector

Window (MeV)	SSM*0.365	7.8/.56/.81	7.7/.56/.80	7.65/.58/.83	7.5/.6/.8	7.0/.54/.71
3.5-7	1592	2480	2407	2434	2371	2027
7-14	3213	3324	3291	3281	3270	3310